INCREASED NOISE EMISSION OF PROPELLERS AND PROPFANS DUE TO PUSHER INSTALLATION

G. Neuwerth, Th. Lölgen, R. Staufenbiel

Department of Aerospace Engineering
RWTH Aachen, University of Technology
5100 Aachen, Federal Republic of Germany

Abstract

The inflow to propellers and Propfans, installed as aft mounted pushers at the fuselage of airplanes, is distorted by wakes of pylons or wings. The increase of the radiated noise because of this installation is investigated theoretically and in experiments for take off and landing configurations. A system of computer codes has been developed to predict the emitted noise fields starting with the distorted flow and calculating steady and unsteady blade forces as a function of the radial position.
For the experimental investigations, a rotor test set was built up in the open test section of a wind tunnel which simulates the flight speed.
The numerous influences on the noise are treated by a parameter study. Measurements of the noise power and spectrum are in good agreement with the theoretical predictions.
Various means for a reduction of the radiated noise have been investigated.

1. Introduction

At cruise Mach numbers up to 0.8, new powerplant concepts for commercial airplanes are based on the use of multibladed propellers, known as Propfans. The development of Propfan propulsion systems is of significant interest due to the high propulsive efficiency. Even for high cruising Mach numbers in the range of 0.8, the specific fuel consumption can be reduced by about 30% compared to current jet engines. However, Propfans provide serious problems with regard to their integration into airplanes. Today, the preferred position of Propfans is the aft-mounted pusher installed in the rear part of the airplanes. As a consequence of this location, the inflow is distorted and leads to an increased noise emission. An additional noise generation arises for all airplane configurations with pusher propellers in the tail region; this also is valid for the airplanes of the General Aviation.

The higher noise radiation of pusher-propellers can be generally explained in the following way. In principle, the noise spectrum of the propeller is dominated by single tones which have the maximum sound levels; they are caused by noise sources located on the rotating blades. Important are sources of dipole type which are related to the blade pressure distributions (s. Kellner (1) and Schreier (2)). Pressures (and forces) on the rotating blades get unsteady for pusher propellers because the inflow to the propellers is disturbed by the wakes of different airplane parts e.g. by pylons. As a consequence, the noise levels of discrete tones, especially at the higher frequencies, are increased. Steep pressure impulses increase the contribution of higher harmonics in the noise spectrum (s. Neuwerth et al. (3)). Thus, the overall sound power level and the noisiness is increased due to the higher frequencies which are more annoying to the human ear.

A rotor test set was built up with devices to generate different well defined distortions in the inflow to the fan. The forward speed was simulated by the flow in the open test section of a wind tunnel.

For the computation of the radiated noise fields, a modular program was built up. Outgoing from flow distortions, the unsteady blade forces and blade pressure distributions were determined and were used as inputs for the noise codes. This program was used to study the influence of different parameters, related to the propellers and to the distorted inflow, on the increase of the radiated noise.

In addition to the principal investigations, various methods of reducing the noise level were studied experimentally. These were active measures which act directly upon the noise sources.

Finally, the noise generation of counter-rotating Propfans was theoretically analyzed for the case of a distorted inflow; it must be taken into account that the blade pressures are already unsteady due to the interaction between the counter-rotating blades.

A lot of papers analyzing the various influences on the noise radiation have been published in the last years (s. Magliozzi (4) or Watanabe et al. (5) for example). This paper is focussed on a deeper insight into the acting mechanisms.

2. The theoretical approach

A system of computer codes has been developed in Aachen in the past years to predict the impulsive noise of rotors with defined disturbances in their inflow (s. Kellner (1), Schreier (2) and Neuwerth (6)). This program system contains several modules for determining unsteady blade forces and pressures as well as the emitted noise field of propellers and Propfans (Fig.2.1). To treat counter rotating propellers, the system was further developed to consider the acoustic and aerodynamic interference between the two rotors.

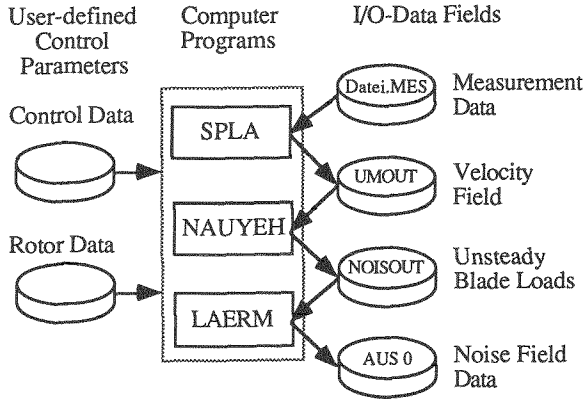

Fig. 2.1 Modular noise calculation program

The first module, SPLA, evaluates the velocity distribution of the inflow, which contains the flow distortions - e.g. the wake of a pylon - and transforms these velocities into the data file UMOUT. This file contains the complete velocity field for the different radial positions of the rotating blades. Using these data, the module NAUYEH determines either the unsteady blade pressures or the equivalent unsteady forces, storing the result in the file NOISOUT. As the last step, the module LAERM calculates the radiated noise field.

2.1 Computation of unsteady blade forces and pressures

Velocity fluctuations at rotor blades occur when the blade passes a flow distortion, e.g. a wake.

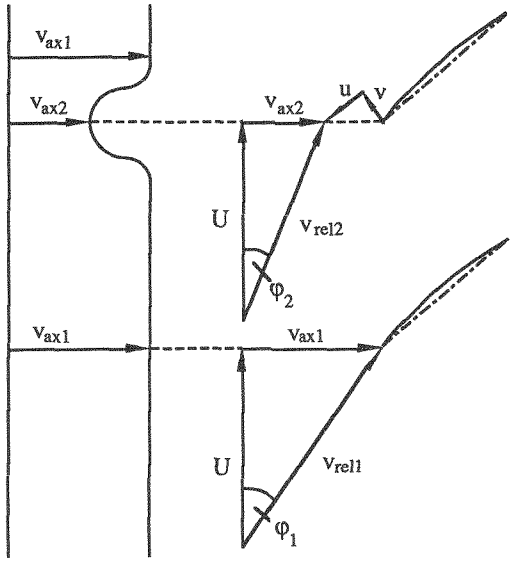

Fig. 2.2 Inflow distorted by a wake

Figure 2.2 illustrates the flow distortions. U is the blade velocity; u and v represent the flow perturbations relative to the blade chord caused by the wake. Primarily, the axial velocity v_{ax} is modified by the wake and its change leads mainly to a variation of the direction of the relative velocity v_{rel} while the change in magnitude is minor. These flow distortions generate blade forces of impulsive shape which causes mechanical vibrations and additional noise radiation.

Starting from the theories developed by Kemp and Sears (7) and Horlock (8), Naumann and Yeh (9) determined the unsteady lift of a cambered airfoil caused by periodical velocity distortions normal and parallel to the blade chord. Compressibility and friction effects as well as interference from neighboring blades were neglected in this approach. The theory is based on singularity methods; the airfoil is represented by a sheet of line vortices located along the chord (Fig.2.3).

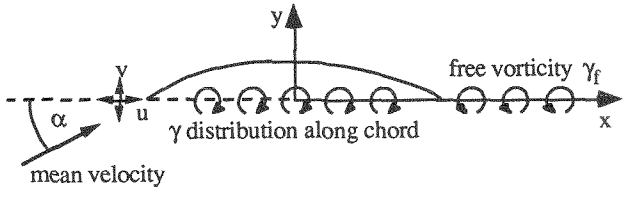

Fig. 2.3 Distribution of vorticity

Since the velocity distortions are periodical for the rotating blades, the inflow can be represented by a mean velocity and the Fourier components of the flow disturbances. Corresponding, the vorticity γ along the blade chord consists of a steady component, γ_{st}, and a time dependent vorticity, γ_{un}:

$$\gamma = \gamma_{st} + \gamma_{un}$$

Because of the variation of the bound vorticity γ_{un}, free vortices γ_f will be shed. These free vortices are assumed to be carried away with the mean velocity along a plane in chord direction. The unsteady vorticities γ_{un} and γ_f induce unsteady velocities at the airfoil. The total flow containing mean flow, disturbances and induced velocities must be tangent to the camber for all x-values. Since the relation between γ_{un} and γ_f is known, an integral equation can be developed connecting the unsteady vorticity γ_{un} to the Fourier-components of the inflow distortions u and v. Applying the Euler equation, the unsteady blade forces can be determined using the computed values of the vorticities.

This theory of Naumann and Yeh was extended by Kellner (1) to compute the unsteady blade pressure amplitudes as well as their phase differences for arbitrary points along the chord. This extension is important if the noise field is computed applying the FWH-equation (s. chapter 2.2.2).

2.2 Theory for determining the radiated sound field

The principles of the theory of noise generation are based on the work of Lighthill (10) who developed the basic general wave equation of the aeroacoustic:

$$\frac{\partial^2 \rho}{\partial t^2} - a_0^2 \frac{\partial^2 \rho}{\partial x_i \partial x_i} = \underbrace{\frac{\partial Q}{\partial t}}_{(1)} - \underbrace{\frac{\partial F_i}{\partial x_i}}_{(2)} + \underbrace{\frac{\partial^2 T_{ij}}{\partial x_i \partial x_j}}_{(3)}$$

This equation contains three different acoustic source terms:

(1) The thickness term (monopole) represents the effect of mass displacement of the rotating blades. The thickness term contributes to the high speed impulsive noise at high tip speeds but it can be neglected at lower tip speeds.
(2) The loading term (dipole) contains the effect of the fluctuating blade forces. These forces are of great importance for the additional noise emission due to a disturbed inflow.
(3) This last term (quadrupole) is equivalent to the effect of turbulent momentum exchange in the boundary layers and the wakes of the blades.

2.2.1 Calculation of the emitted noise field as a function of unsteady blade forces

The part of the computer program which determines the sound power level uses the unsteady blade forces as input. The only acoustic source term regarded is the dipole source term; the other source terms are neglected. Under these conditions, a solution of the wave equation was developed by Lighthill in the form:

$$p_s = -\frac{1}{4\pi} \frac{\partial}{\partial x_i} \int \left[\frac{F_i}{d}\right]_{ret} dA$$

where p_s is the sound pressure at the position of the observer while d is the distance between the source Q and the observer. dA is an element of the rotor area and F_i are the components of the force per unit area acting on fixed points in the rotor area. F_i is generated as the reaction of lift and drag of the rotor blades. The square brackets around F_i/d imply the evaluation at the retarded time $\tau=t-d/a_o$. The integration over the rotor area is performed in parts over the radius R_t and the azimuth angle ψ. The notations are given in figure 2.4.

For an undisturbed inflow the blade forces do not change during a rotor revolution. For a fixed point in space, however, the F_i fluctuate every time a blade passes by, as illustrated in figure 2.5. Consequently, these fluctuations are periodical with the blade passing frequency B*n, where B is the number of blades and n is the rotor rotational speed.

Because of their periodicity, these fluctuations can be Fourier-analyzed with the discrete frequencies $f_m=m*B*n$ where m is the harmonic order. The Fourier-coefficients depend on the shape of the F_i-pulses which, on their part, are determined by the pressure distribution on the blade elements.

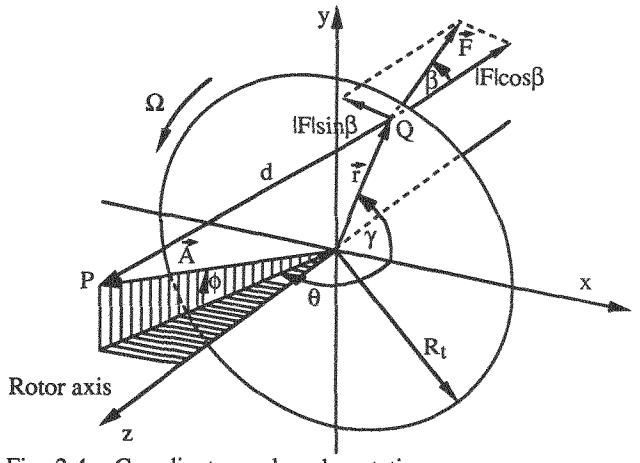

Fig. 2.4 Coordinates and angle notations for the noise calculation program

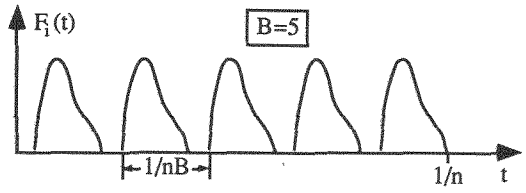

Fig. 2.5 Fluctuation of F_i at a fixed point in space near the rotor area

In case the inflow is distorted, the blade forces K are not constant any longer during one revolution, but are periodical with the frequency k*n, where k is the number of impulsive disturbances which pass the blade element during one revolution. Therefore K can be Fourier-analyzed resulting in the Fourier-coefficients K_l and the discrete frequencies $f_l=l*k*n$ where l is the harmonic order.
The forces K(t) lead also to fluctuations of $F_i(t)$ at a fixed point in space. In fact, every force-harmonic K_l generates a fluctuation F_{il} which in turn is periodical and can be Fourier-analyzed at the discrete frequencies $f_m=m*B*n$. Consequently every single blade force-harmonic generates series of F_i- and sound pressure harmonics.

For determining the radiated noise of the entire rotor, the contributions of all points in the rotor area have to be integrated considering their phase relations. The dependence of the Fourier-components and their phase relations on the radial position required an extension of the existing rotor noise theories of Lowson (11), Ollerhead and Munch (12) and Wright (13). This was done by Schreier (2). He deduced the following equation for the sound pressure harmonics p_m:

$$p_m(t,\phi,\theta) = \frac{B}{4\pi A}\int_0^{R_t} \frac{1}{r} * |\chi(mB,r)| * \sum_{l=0}^{\infty} K_l(r) *$$

$$\{ J_{q_-}\left(mB\Omega\frac{r}{a_0}\cos\theta\right) * \left(mB\Omega\frac{r}{a_0}\sin\theta\cos\beta - q_-\sin\beta\right)$$

$$* \sin\left(mB\Omega\left(t-\frac{A}{a_0}\right) - q_-(\phi-\pi/2) - \varphi_l(r)\right)$$

$$+ J_{q_+}\left(mB\Omega\frac{r}{a_0}\cos\theta\right) * \left(mB\Omega\frac{r}{a_0}\sin\theta\cos\beta - q_+\sin\beta\right)$$

$$* \sin\left(mB\Omega\left(t-\frac{A}{a_0}\right) - q_+(\phi-\pi/2) + \varphi_l(r)\right) \}dr \,.$$

The amplitudes of the blade force harmonics K_l and their phase differences φ_l can be evaluated by the above described procedure. q is the modal order of the sound field with $q_+=m*B+k*l$ and $q_-=m*B-k*l$. Ω is the angular velocity of the rotor, J_q is the Bessel-function of the q^{th} order. χ is a spectral function determining the pressure distribution along the blade chord. It is assumed that the normalized pressure distribution is not time dependent.

For comparison purposes with measurements in the reverberation room of the wind tunnel (s. chapter 3), the sound power level PW_m was computed by integrating the square of the RMS-values of p_m over a sphere around the rotor:

$$PW_m = \frac{1}{T} * \int_{t=0}^{T}\int_{\phi=0}^{2\pi}\int_{\theta=0}^{2\pi} \frac{p_m^2(t,\phi,\theta)}{\rho_0 a_0} d\theta\, d\phi\, dt$$

2.2.2 *Calculation of the emitted noise field using the FWH-equation*

The inhomogeneous wave equation of Lighthill was extended by Ffowcs-Williams and Hawkings for moving sound sources. This is of great importance for the calculation of directivity characteristics. The Ffowcs-Williams/Hawkings-equation (FWH-equation) can be written as:

$$4\pi p(t,\phi,\theta) = \frac{\partial}{\partial t}\int_S \left[\frac{\rho_0 V_n}{r|1-M_r|}\right]_{ret} dS(\vec{y})$$

$$+ \frac{1}{a_0}\frac{\partial}{\partial t}\int_S \left[\frac{P_r}{r|1-M_r|}\right]_{ret} dS(\vec{y})$$

$$+ \frac{1}{a_0^2}\frac{\partial^2}{\partial t^2}\int_V \left[\frac{T_{rr}}{r|1-M_r|}\right]_{ret} dV(\vec{y})$$

The right hand side of the equation contains again the three acoustic source terms monopole, dipole and quadrupole. The latter term was neglected again. To get the noise-directivity characteristic in a reverberation room, measurements have to be made in the acoustic nearfield of the rotor. Therefore, a dipole nearfield term was added in the mathematical model:

$$\int_S \left[\frac{P_r}{r^2|1-M_r|}\right]_{ret} dS(\vec{y})$$

In the FWH-equation, $p(t,\phi,\theta)$ is the sound pressure at the observer position for the time t. The sound pressures of the different sources at y have to be integrated for the retarded time τ (s. below). M_r is the Mach number of the source velocity component and P_r the local blade pressure component in the direction of the observer, while V_n is the velocity component normal to the chord (Fig.2.6). The Doppler-factor $1/|1-M_r|$ contains the movement effect of the noise sources.

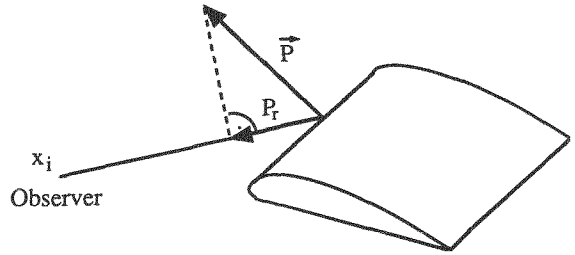

Fig. 2.6 Effective blade pressure in the direction of the observer

For the calculation of the monopole term, the velocity components normal to the blade chord, the mass displacement, has to be computed for each panel. To obtain the dipole term, the local blade pressures at the rotor blades are needed. The

unsteady blade pressures are calculated with the code described above.

The sound which arrives at the time t at the observer position has been radiated from the position of a blade element at the retarded time τ (Fig.2.7).

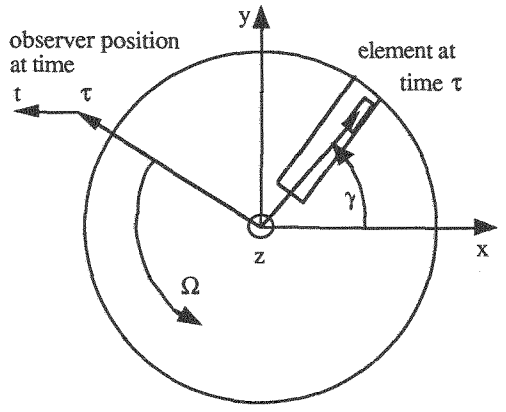

Fig. 2.7 Relation observer - element at times t and τ

3. Rotor test set

The rotor test set consists of a model of the airplane Fantrainer, a product of the Rhein Flugzeugbau GmbH. The propulsion system of this airplane, an integrated ducted fan, is scaled 1 : 2 (Fig.3.1).

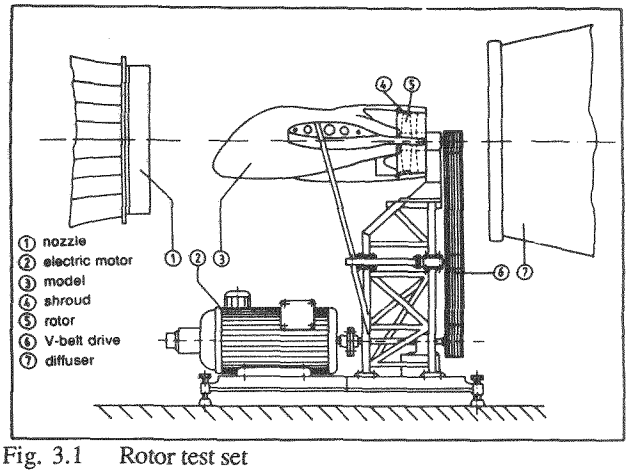

Fig. 3.1 Rotor test set

The 5-bladed rotor has a diameter of 0.60 m and a shroud length of 0.32 m. The rotor blades have a radial length of 0.18 m and a chord length of 0.08 m. The rotor speed is limited to 5500 1/min.
The test set was installed in the test section of a subsonic wind tunnel where flight speeds v_∞ can be simulated in the range up to 70 m/s.

The inflow of the rotor is distorted by four wakes generated by the left and right side of the wing and by the upper and lower strut of the shroud. The velocity profiles of the wakes were changed by different means. 2 D measurements of the flow were conducted upstream and downstream of the rotor using a split-fiber-film probe.

Since the room, which surrounds the wind tunnel, is a reverberation room, the sound power of the propeller could easily be calculated by a proven method described by Kellner [1]. The noise-directivity characteristic was measured in the acoustic nearfield inside the wind tunnel flow with a special microphone.

4. Theoretical and experimental results during take off and landing

4.1 Parameter study of the noise emission

Beside the velocity distortions of the rotor-inflow, further rotor parameters as diameter D, number of blades B, revolutions per minute n and lift coefficient of the blades c_L have influence on the emitted noise power. The special influence of the inflow distortions - here the wakes of pylons or wings - is the main topic of this paper. Therefore, shape and strength of the wakes were changed at first, and their influence on the radiated noise power levels was investigated theoretically in a systematic parameter study. The other parameters were chosen corresponding to takeoff and landing conditions.

During one revolution, every blade interacts with one wake. The shape of the wake can be described by three characteristic parameters, the amplitude A (difference between v_∞ and the minimum axial velocity in the center of the wake), the maximum gradient G of the velocity profile and the loss of momentum I_0 in the wake.
The analysis reveals that the gradient G is of little influence on the radiated noise. For constant values of A and I_0, the gradient can be changed independently if the wake is specially modeled. The variation of G is done in the way shown in figure 4.1. Outgoing from a given width of the wake, the lowest G is obtained for a triangular shape, whereas trapezoidal forms have higher G values. As the gradients, realized in the measurements, are in a range from 200 to 1500 1/s, the theoretical results are shown for this range in figures 4.2 and 4.3. Thereby, the loss of momentum I_0 and the amplitude A were chosen I_0 = 100 N/m and A = 20 m/s corresponding to the values occurring in our measurements.

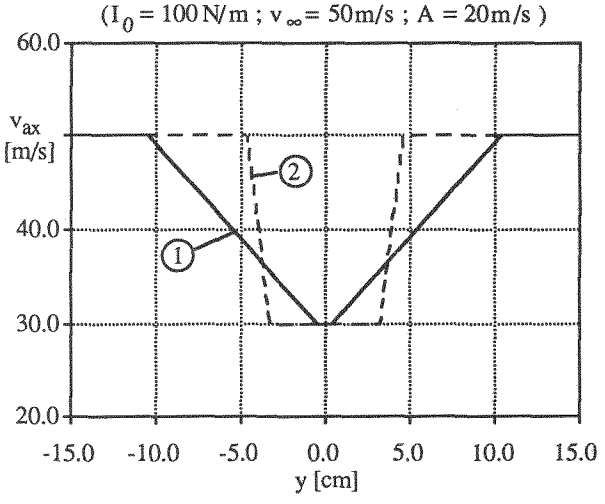

Fig. 4.1 Modeling of the wakes with trapezoidal form

Some results of the calculation are shown in figure 4.2 and 4.3. Even though the gradient G varies over a wide range, the total emitted noise power level OAPWL is only slightly influenced. For the data of the rotor test set (D = 0.6 m) the variation of the OAPWL is in the range of not more than 2 dB (Fig.4.2), while for a rotor diameter in the size of the original airplane Fantrainer (D = 1.2 m) and the rotational tip Mach number 0.74 the variation of the OAPWL remains within 0.5 dB. The low sensitivity to the gradient can be explained in the following way. With growing values of G the Fourier-coefficients of the axial velocity distribution decrease for lower harmonics and increase for higher harmonics. The unsteady blade force harmonics behave correspondingly. Since the higher force harmonics have only a lower influence on the noise power, the OAPWL-values can even be diminished for high gradients (Fig.4.3).

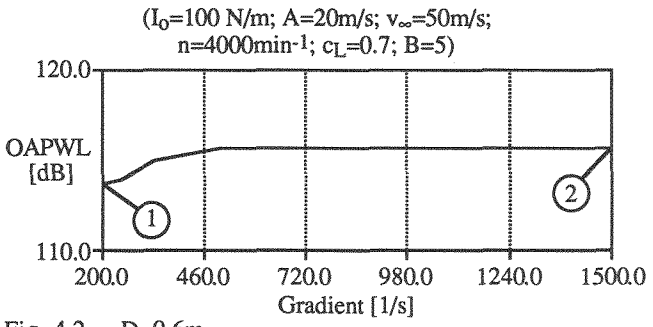

Fig. 4.2 D=0.6m

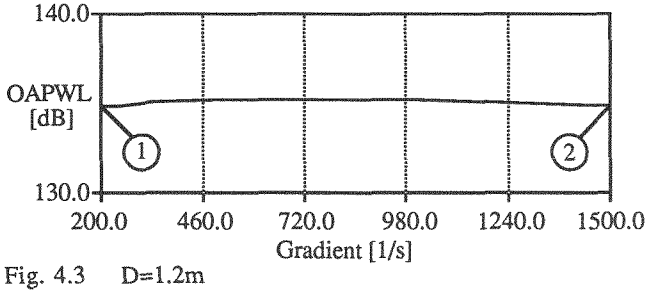

Fig. 4.3 D=1.2m

Sound power level as a function of the velocity gradient of the wake profile

Therefore, the influence of G can be neglected and only two parameters of the wakes must be considered, A and I_0. As a consequence, the wake profiles can be modeled using an uniform shape. It was found that measured wake velocity profiles can be approximated fairly well by a Gaussian distribution. In figure 4.4, a fitting of the velocity profile, measured in our test set, is presented. Although the measured wake of the wing is not quite symmetric - the gradient of the wake on the suction side (positive y-values) is smaller than on the pressure side - the approximation is satisfactory.

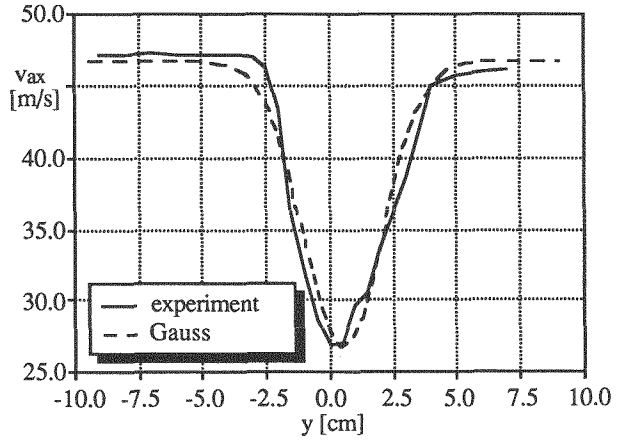

Fig. 4.4 Comparison of a Measured Wake of the Wing with a Bell Shaped Gaussian Wake

Basing on modeled wakes, the influence of variations of A and I_0 was analyzed for four different rotors

- the rotor used in the test set, D = 0.6 m leading to a rotational tip Mach number of M_t = 0.37 (case A),
- the rotor of the Fantrainer, D = 1.2 m and M_t = 0.74 (case B),
- the same rotor with D = 1.55 m and M_t = 0.95 (case C),
- a rotor with D = 1.55 and 10 blades instead of 5 (case D) (this rotor is similar to a single rotating Propfan, further details s. chapter 5).

All rotors have the same flight speed v_∞ = 50 m/s and rotational speed n = 4000 /min. The lift coefficient is constant (c_L = 0.7) for all radial parts of the blades.

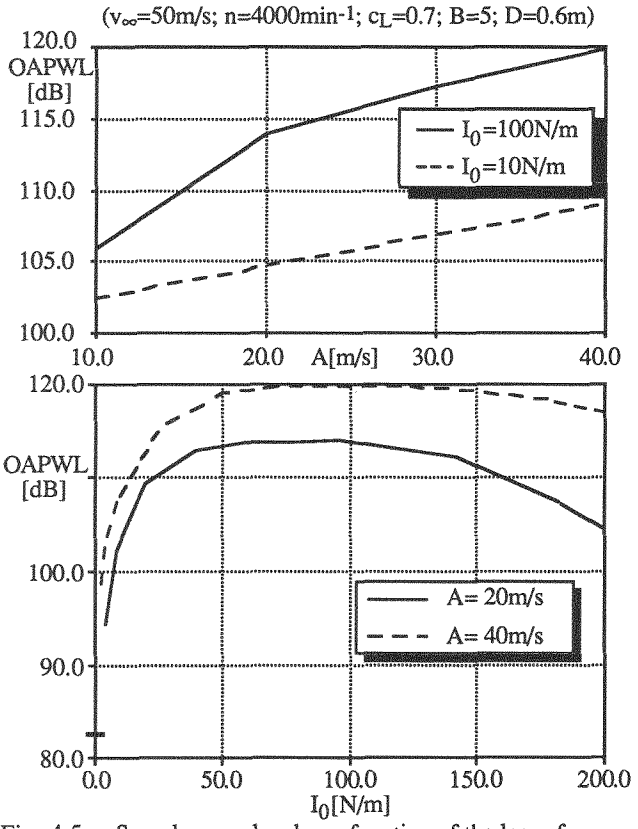

Fig. 4.5 Sound power level as a function of the loss of momentum in the wakes and of their amplitudes (case A)

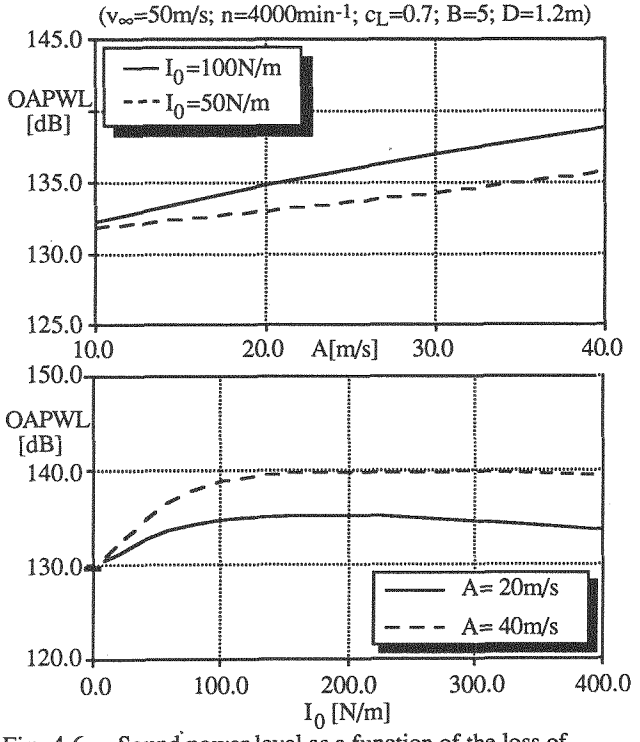

Fig. 4.6 Sound power level as a function of the loss of momentum in the wakes and of their amplitudes (case B)

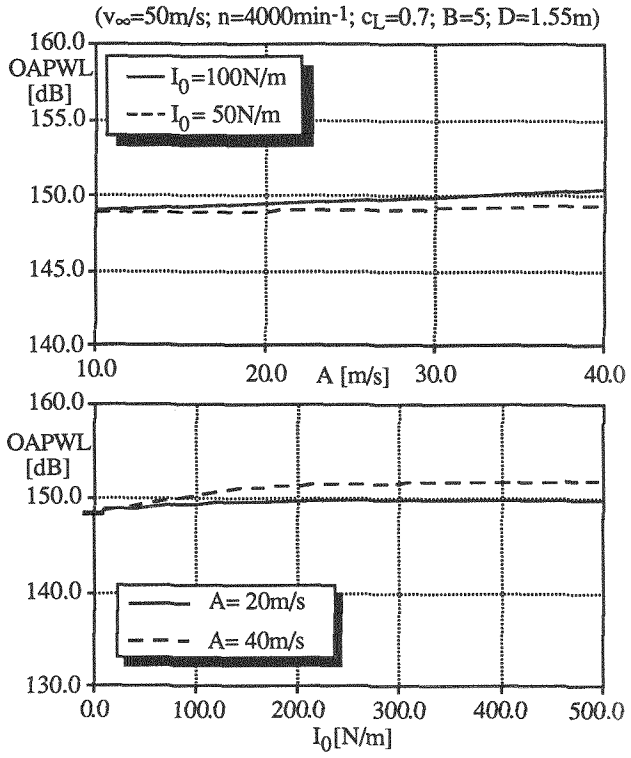

Fig. 4.7 Sound power level as a function of the loss of momentum in the wakes and of their amplitudes (case C)

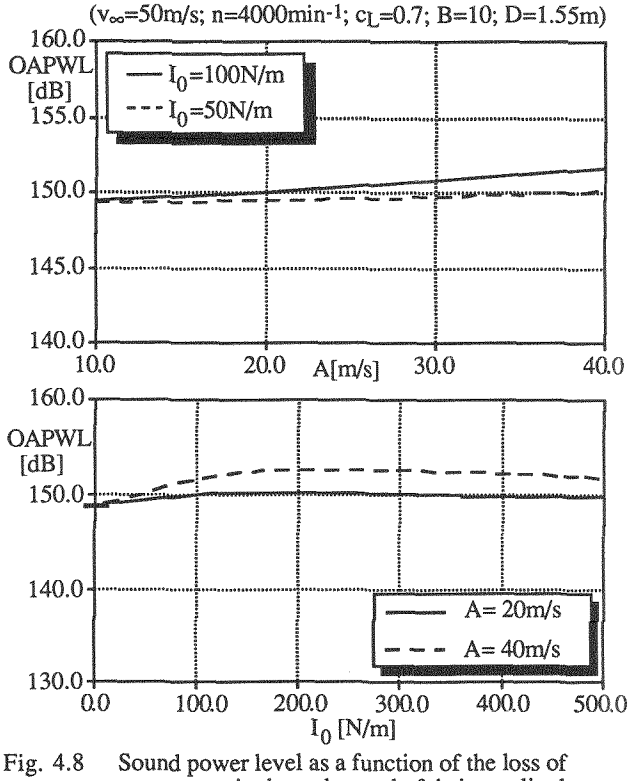

Fig. 4.8 Sound power level as a function of the loss of momentum in the wakes and of their amplitudes (case D)

The results for the four cases are shown in the figures 4.5 to 4.8. In the lower part of each figure the influence of I_0 on the OAPWL for two different amplitudes, A = 20 m/s and A = 40 m/s, is plotted while in the upper part the influence of the amplitude is analyzed for two different values of I_0. For case A, representing the smallest rotational tip Mach number (M_t = 0.37), the curves in the lower plot of figure 4.5 start at I_0 = 0 with a low value of OAPWL = 83 dB. Here no wake exists and the blade forces are steady. For growing wakes the OAPWL rises very rapidly. At I_0 = 10 N/m the OAPWL has already reached 104.5 dB (A = 20 m/s) and 109 dB (A = 40 m/s), respectively, and is turned in saturation, at about I_0 = 50 N/m, with an OAPWL of more than 30 dB above the undisturbed case. When I_0 has values of about 100 N/m the OAPWL reaches maximum values of 114 dB and 120 dB respectively. The strength of the wakes with I_0 = 100 N/m and A = 40 m/s is in the upper range of that wakes occurring in our measurements; those wakes are increasing the OAPWL up to 37 dB compared with a homogeneous inflow.

This comparably strong influence of inflow distortions on the sound power level can be explained by the fact that the noise level due to steady blade forces is small in this case because of the very low values of the Bessel-function for low tip Mach numbers M_t. The Bessel-function is an important factor in the equation for determining the sound pressure (s. chapter 2.2.1). The physical meaning of this function is to consider the interference of the sound waves outgoing from the sources in the rotor area. For steady forces, the Bessel-function

$$J_{mB}\,(mB\,M_t \cos\theta)$$

has maximum values at the blade tip for m = 1 (blade passage frequency) and for the angle $\theta = 0^o$ (observer in the rotor area). The maximum value is obtained for $J_5(1.85) = 0.0049$, while for some blade forces harmonics the Bessel-functions reach maximum values up to 1.0.
In case B (M_t = 0.74; D = 1.2 m), the maximum value of the Bessel-function increases to $J_5(3.7) = 0.1$ for the steady forces. Thus, the Bessel-functions for the unsteady blade forces differ less from the steady case and the steady forces get much more influence on the sound pressure. The difference between the undisturbed and the disturbed case is further reduced because the fluctuations of the angle of attack $\Delta\alpha$ get smaller, for constant amplitudes A, if the larger rotor diameter leads to a higher blade tip speed ($\Delta\alpha$ is approximately proportional to A/M_t). These facts are causing a reduction of the influence of inflow distortions on the radiated noise power for higher rotational tip Mach numbers M_t. This influence can also be seen by comparing case B in figure 4.6 with case A in figure 4.5. For I_0 = 0 (steady blade forces), the OAPWL is increased to 120 dB from 83 dB for case A. But the maximum increase of the OAPWL in case B due to the wake is only 5 dB (A = 20 m/s) respectively 10 dB (A = 40 m/s).
At values of I_0 which differ by a factor of 2 in case A and B, the wakes cover the same portion of the rotor circumference πD and the velocity fluctuations at the blades have the same spectrum. Thus, the unsteady aerodynamic effects must be the same (the reduced frequencies ω are identical) leading to the same spectral distribution of the unsteady blade forces.

The effects of the different force-harmonics K_l on the noise power are shown in figure 4.9 for the rotor diameters of D = 0.6 m and D = 1.2 m. To achieve nearly the same values for the fluctuations of the angle of attack, $\Delta\alpha$, the amplitudes of the wakes were selected as 20 m/s and 40 m/s for D = 0.6 m and 1.2 m, respectively. To obtain the same spectral distributions of the unsteady blade forces, the values of I_0 were selected as I_0 = 60 N/m and 120 N/m for the different diameters.

The spectral distributions of the unsteady forces per radial length (Fourier-coefficients K_l) are plotted in the lower part of figure 4.9 for the radial position of 80% of the blade tip radius R_t (the K_l-values have to be computed for several radial positions). It reveals that for both diameters the decrease for higher harmonics is practically the same. The force level is much higher for the larger D because of the doubling of the

maximum tip speed and of the chord length of the blades. Correspondingly, also the steady forces are higher in case B (3297 N/m at r/R_t = 0.8) compared to case A (513 N/m at r/R_t = 0.8) and they are much stronger than the unsteady forces. In the upper part of figure 4.9 the contribution of the force harmonics l to the noise power level PWL is shown for the different sound harmonics m.

For case A, the steady blade forces (l = 0) contribute most to the blade passage frequency (m = 1), but the level is comparatively low with PWL = 83.3 dB because of the very low value of the Bessel-function. The contribution to higher sound harmonics is still less and too low to have any influence on the noise level. According to figure 4.5, the unsteady blade forces generate much higher levels. The strongest contribution to the blade passage frequency (m = 1) is provided by the 5th force harmonic (l = 5). The 1st sound harmonic (m = 2) is mostly influenced by l = 9 while l = 13 gives the highest contribution to m = 3. All sound harmonics together generate a level of 113.7 dB which is identical to the OAPWL because of the negligeable contribution by the steady blade forces.

For case B, the increased influence of the steady blade forces can be taken from figure 4.9. The level generated by the steady blade forces is now in the same order of magnitude as the contribution from the unsteady blade forces (about 130 dB). An increased number of force harmonics l brings now a relatively strong contribution to every sound harmonic m. The OAPWL computed with this multitude of high levels in the sound spectrum is 139.7 dB. For both cases, A and B, the blade force harmonics, which are of influence on the OAPWL, are in the range from l = 1 to l = 15. While a rotor with constant blade forces has a spectrum whose higher harmonics steeply decrease, a disturbed inflow can generate many sound harmonics with nearly equal levels which all contribute to an increasing OAPWL.

In case C (Fig.4.7), the rotational tip Mach number is increased to M_t = 0.95 by enlarging the rotor diameter to D = 1.55 m. Thus, the steady blade forces have a further amplified influence on the sound power levels, the contribution of the unsteady blade forces to the OAPWL is, with less than 3 dB, marginal. For I_0 = 0, the OAPWL amounts now to 148.8 dB caused by high values as well of the Bessel-functions as of the steady blade forces. The Bessel-functions for the unsteady blade forces are increased only slightly and their force amplitudes are influenced by a decrease in $\Delta\alpha$.
Figure 4.8 gives results for case D where the number of blades is increased to 10. Compared to case C, the OAPWL is slightly more influenced by the unsteady blade forces. This can be explained by somewhat smaller Bessel-functions for the steady forces.

As a next step, the influence of the wake amplitudes A is considered (upper parts of the figures 4.5 to 4.8). It can be seen that the influence of A is reduced if M_t increases (from case A to C).
The following statement can be made: if the sound power level is highly influenced by the unsteady blade forces, the OAPWL is increased in a strong way by I_0-enhancement as well as by A-enhancement. Actually for small I_0-values the influence of I_0 predominates while for high I_0-values the influence of A predominates.

If not the rotor diameter would be increased as done above but the rotor revolutions per minute, then in principle the same statements with nearly the same tendencies can be made. Of course the numerical values would be different.

4.2 Noise emission of selected test configurations

Using the test set (chapter 3), tests were performed with the rotational speed n as a parameter keeping the following parameters constant: B = 5; D = 0.6 m; v_∞ = 50 m/s and

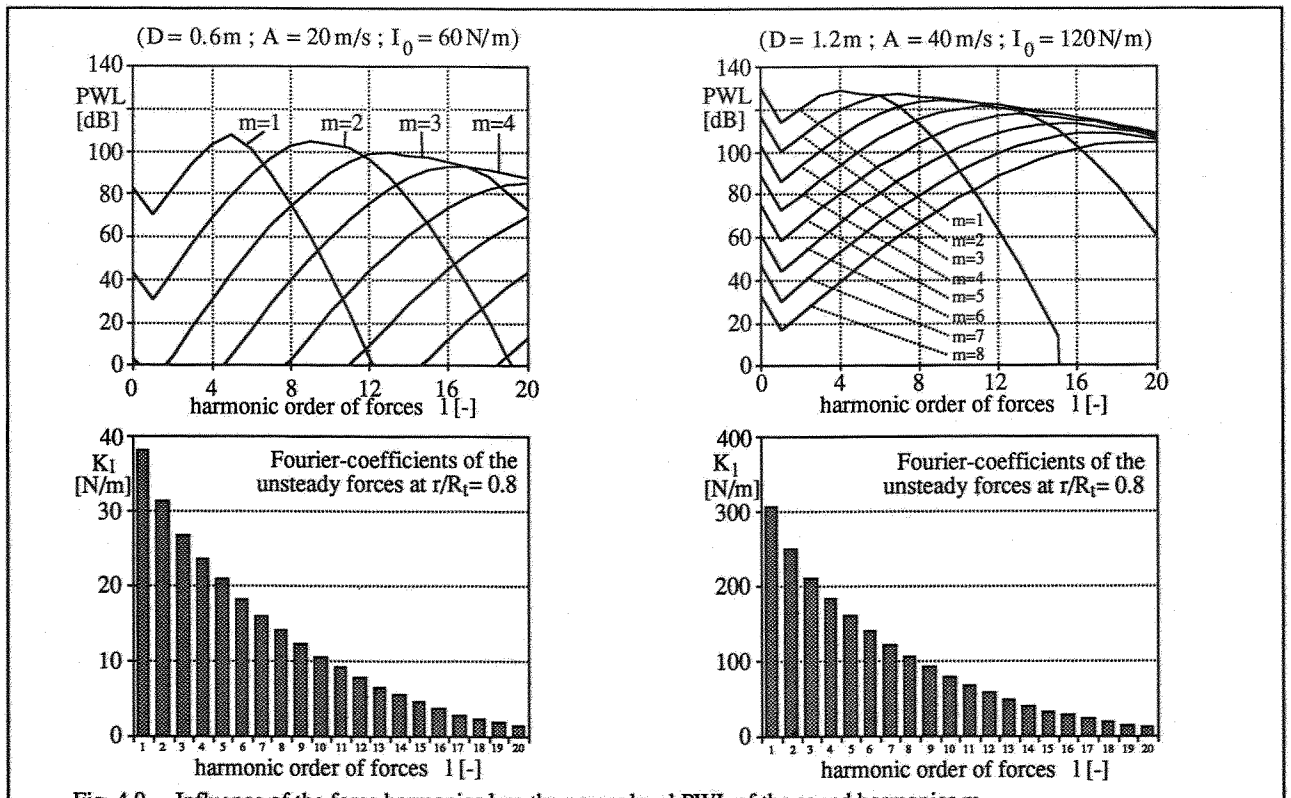

Fig. 4.9 Influence of the force harmonics l on the power level PWL of the sound harmonics m (v_∞=50m/s; n=4000min^{-1}; c'_L=0.7; B=5)

α_{eff} = 7°.The rotor had the constant value of α_{eff} = 7° for its outer radial parts which are mainly responsible for the total thrust and the noise emission; α_{eff} = 7° is equivalent to a lift coefficient of c_L = 0.7. To keep α_{eff} constant, an increase of the rotational speed was compensated by a decrease of the blade angle. Under this condition, the blade forces and the rotor thrust are proportional to n^2.

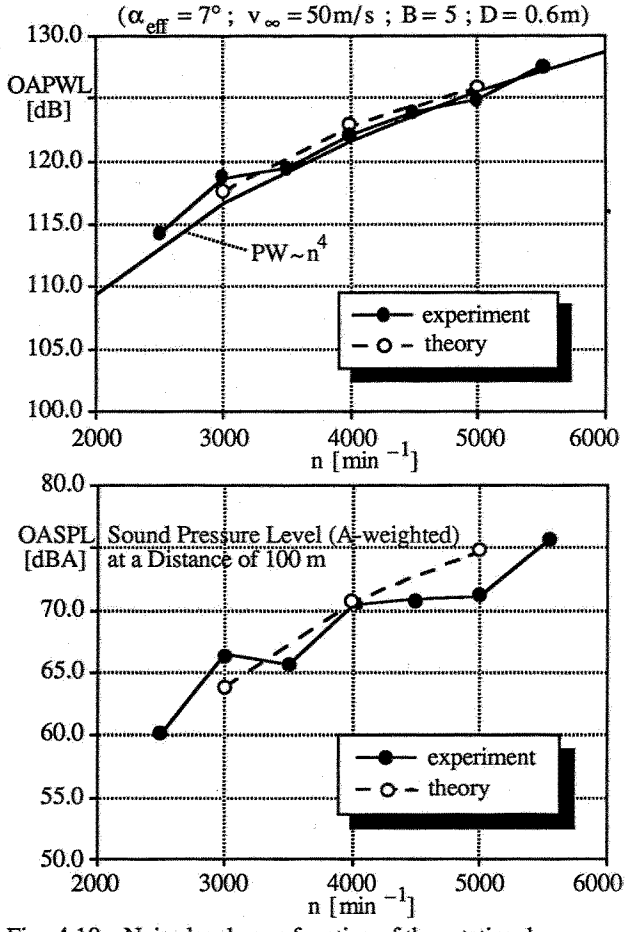

Fig. 4.10 Noise levels as a function of the rotational speed for constant effective angle of attack

The sound power levels are plotted in figure 4.10. Comparing the OAPWL-values with those in figure 4.5 (n = 4000 min^{-1}), it can be seen that they are higher. This can be explained by the fact, that the inflow is now distorted by four wakes generated by the left and right wing and the wakes of the upper and lower strut. The profiles just in front of the rotor are shown in figure 4.11.

The theoretical results (the theory was described in chapter 2.2.1) are in good agreement with the experiment. The effect of the propeller shroud was not considered in the calculation of the emitted sound; obviously the shroud has only a slight influence for the configuration used here. With increasing rotational speed n the OAPWL is raised; the sound power PW is here proportional to about n^4. For comparison, a curve characterising this dependence is plotted in the figure. The exponent "4" is lower than the value for a rotor with homogeneous inflow. This can be explained by the fact that the Bessel-functions for the unsteady blade forces increase only slightly with growing n. Furthermore, the amplitudes of the unsteady forces are only proportional to n because $\Delta\alpha$ is approximately proportional to A/M_t.

The spectral distribution of the radiated sound pressure level is shown in figure 4.12 (where in the upper part the experimental and in the lower part the theoretical results are presented).

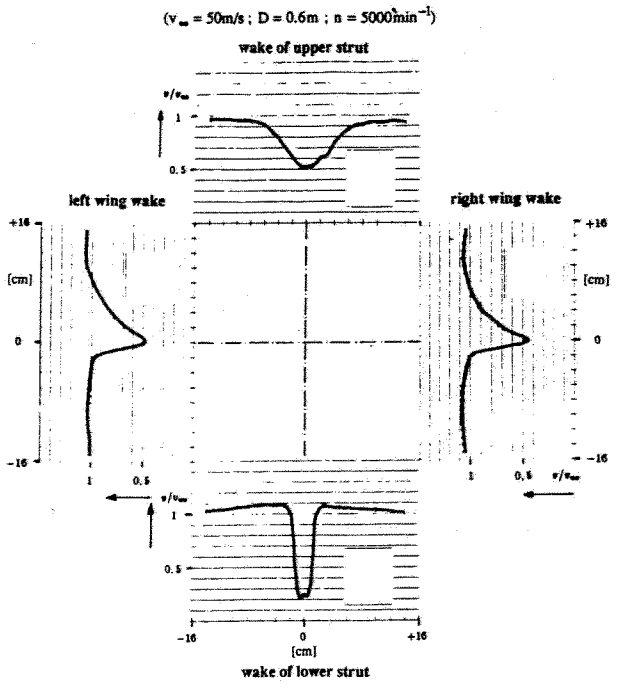

Fig. 4.11 Distorted inflow to the propeller

The spectral distribution of the radiated sound pressure level is shown in figure 4.12 (where in the upper part the experimental and in the lower part the theoretical results are presented).

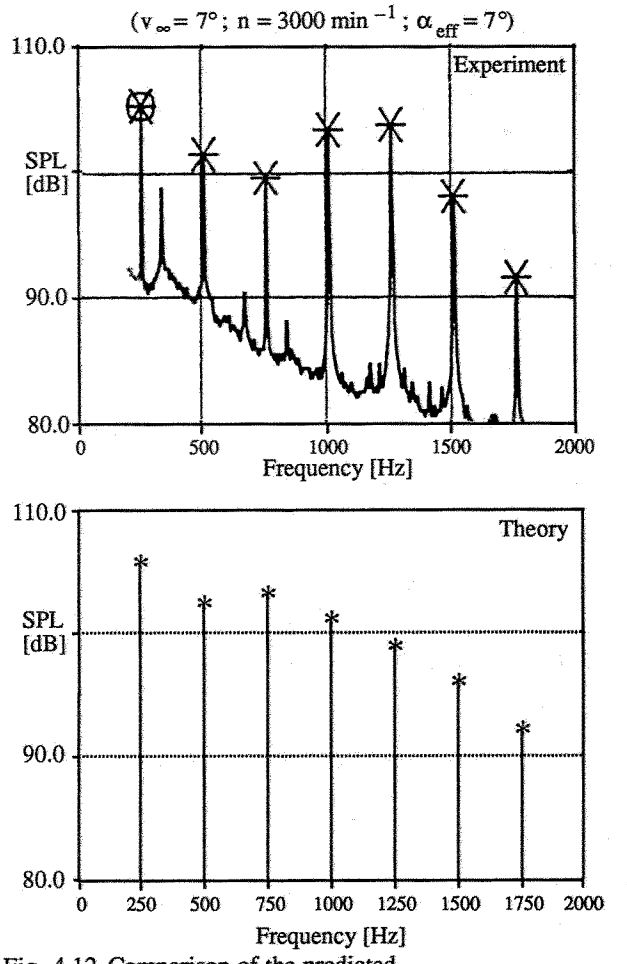

Fig. 4.12 Comparison of the predicted and measured noise spectrum

In contrast to a propeller with homogeneous inflow, the spectrum decreases only slowly for higher sound harmonics. This is characteristic for a propeller with disturbed inflow as explained before. At the blade passage frequency (f = 250 Hz) and at the first harmonic, the computed and measured levels agree very well while for higher harmonics small differences occur.

In the lower part of figure 4.10 the overall sound pressure levels OASPL are shown for an observer in a distance of 100 m from the propeller outgoing from the sound power levels in the upper part . The OASPL-values are weighted with the A-filter to account for the frequency-dependent characteristic of the human hearing. With increasing n, the levels rise faster than the power levels because the frequencies of the radiated tones become higher and thus more annoying.

As next, the sound power levels of the rotor of figure 4.10 were analyzed for constant propeller thrust. In these tests, the effective angle of attack was reduced for increasing n. The test runs were performed for two constant blade forces, 210 N and 440 N (Fig.4.13).

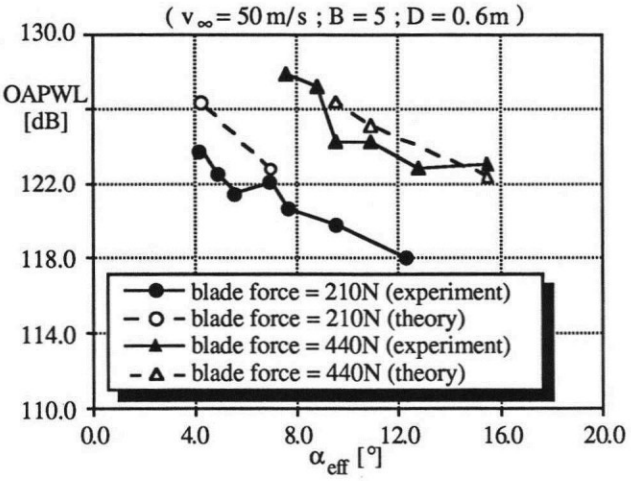

Fig. 4.13 Sound power level as a function of the effective angle of attack for constant rotor thrust

It is obvious that, in general, the noise decreases with increasing α_{eff}. That means, it is favourable to choose high angles of attack and low blade tip speeds. This tendency was already described by Magliozzi [4]. It is, of course, to be expected that for still higher values of α_{eff} the noise levels will increase.because the aerodynamic efficiency of the rotor decreases and the flow will partly separate. In figure 4.13 also the computed sound power levels are plotted. They are again in good agreement with the experiments. As an important input for the theory, the distorted inflow, containing the four wakes, was investigated experimentally. Thereby, the wakes depend on α_{eff} and/or n.

4.3 Methods to reduce the interaction noise

Several methods for reducing the radiated noise power have been investigated in earlier studies by wind tunnel test and even flight tests with the Fantrainer (s. Kellner [1]; Neuwerth et al. [3]).

A successful method of reducing interaction noise, caused by wakes, is the employment of propellers with swept blade shape. Here, the aim is not the improvement of the aerodynamic efficiency in the higher Mach number range, as intended by using Propfans, but to spread the interaction of a blade with a wake over a longer period of time. That means that the several radial parts of the blade interact at different times with the wake. In this way, the impulsive character of the sound radiation is changed and the higher harmonics in the sound spectrum are reduced. This kind of propellers were tested in our wind tunnel as well as in flight test with the Fantrainer. In both investigations, the result revealed a reduction of the OAPWL in the order of 3 dB, for constant thrust, D = 0.9 m and M_t in the range of 0.5. For further details see Kellner [1].

Other ways for noise reduction intended to reduce A and/or I_o of the wakes for a given pylon or wing. Several methods were investigated in experiments:
In a first appoach, air was blown out from the trailing edge of the wake-generating body to fill the wake. The injection had to be done very carefully to achieve a smooth wake profile. Otherwise, the interaction noise can even be increased

A second method used vortex generators at the surface of the wake-generating body to reduce the value of A by intensifying the mixing prozess in the boundary layer. We were, however, not successful to reduce the noise by this method.

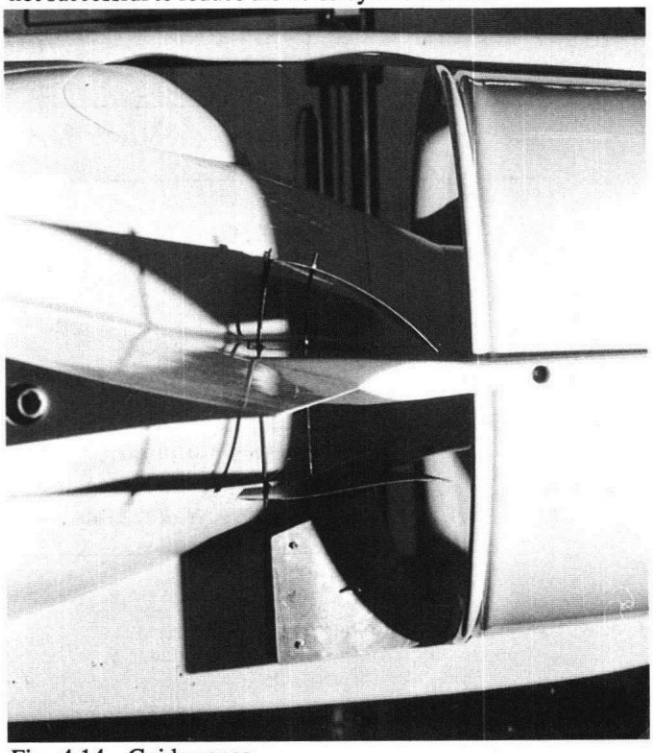

Fig. 4.14 Guide vanes

Another arrangement used guide vanes to bring air with high kinetic energy into the wake to accelerate the flow. Figure 4.14 shows these vanes mounted just before the trailing edges of the wing and the struts. The design of the geometry of the vanes must be done very carefully because every vane generates its own additional wake. The best results were obtained when mounting a single guide vane at each trailing edge at that side where the blades run to. In this way, the additional possibility was given to turn the flow inside the wakes into the direction of the rotating blades so that the flow in the wakes attained a higher swirl. The swirl inside the wakes leads to a decrease of the fluctuations as well of α_{eff} as of the unsteady blade forces. Using the rotor test set, a reduction of ΔOAPWL = 1.5 dB was achieved.

Much more complicated was the method to suck the boundary layer of the wing in front of the rotor for reducing A and I_o. For this purpose, the surface of the wing at the suction and the pressure side was perforated with small holes in a determined way. Inside the wing a low pressure chamber was installed which was connected to a compressor to maintain the necessary underpressure. It is favourable to suck more mass per time in

the forward part than in the rear part of the wing surface. Therefore, the number of holes per surface area increases from the trailing to the leading edge. Figure 4.15 shows the wakes of the wing with and without suction. The wake could be diminished to a high degree. Only a small wake remained because the trailing edge of the wing in front of the rotor is relatively thick for structural reasons.

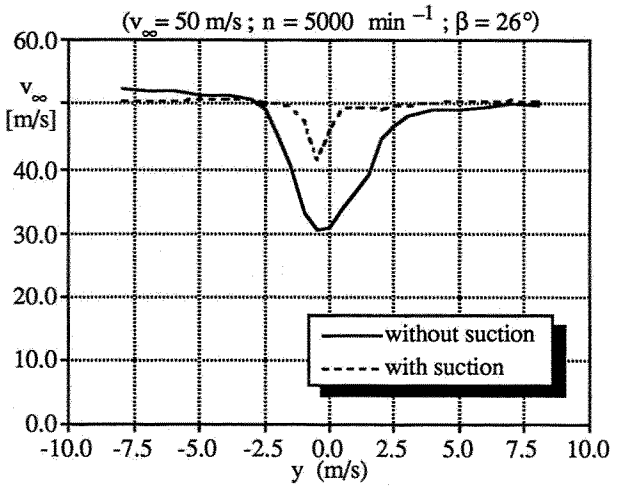

Fig. 4.15 Wake influenced by boundary layer suction

The reduction of the OAPWL can be seen in figure 4.16. It compares the levels with and without suction (Fig.4.10). The reduction increases with the rotational speed and amounts to 3.5 dB for n = 5540/min. These relatively small reductions are understood because the strong wake of the lower strut dominates now (Fig.4.11). This wake could not be sucked because of the inner structure of the strut. The reductions in figure 4.16 are in good agreement with the calculations.

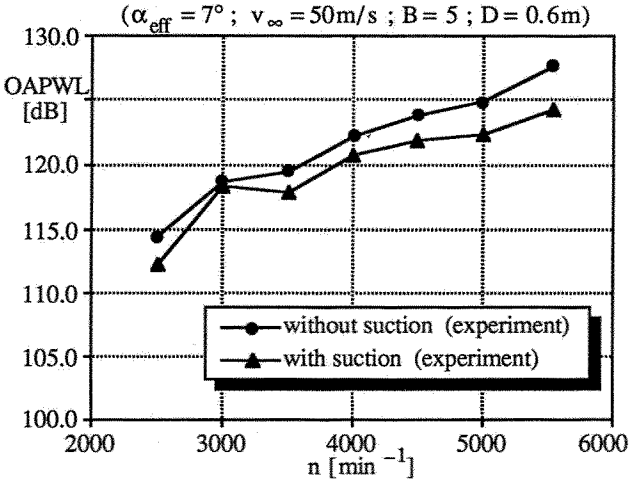

Fig. 4.16 Sound power level as a function of the rotational speed for constant effective angle of attack

4.4 The circumferential directivity characteristic

Using the test set, the circumferential noise directivity characteristic of the rotor was measured in the acoustic nearfield. A microphone was moved on a circle with a diameter of 0.8 m concentric to the rotor and 0.27 m in front of the rotor area. In figure 4.17 the measured sound pressure levels, SPL, for the blade passing frequency (m = 1) and the 2nd harmonic (m = 3) are plotted as a function of the circumferential angle. The angle, labeled 0°, is vertical above the aircraft. Looking from behind, the rotor rotates counter-clockwise. This means the rotor interacts with the wake of the left and right side of the wing at 90° and 270° respectively, and with the wakes of the upper and lower struts at 0° and 180° respectively.

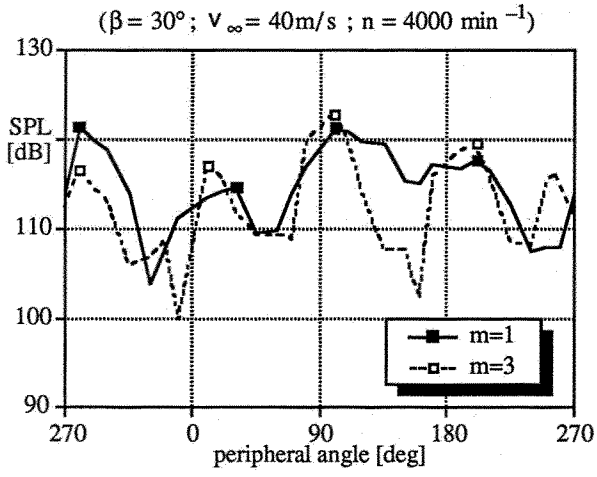

Fig. 4.17 Circumferential directivity pattern

The slopes of the directivity patterns show four maximum levels marked in the figure. These maxima are related to the four wakes. Their levels are about 10 dB higher than the levels of the neighboring minima. For a propeller without a shroud this tendency would be even stronger. Additionally can be seen, that the sound is correlated to the wake positions. The noise pattern of the propellers, given by the maximum of the SPLs, shows that the noise radiation is turned, relative to the position of the wakes, by more than 10° into the direction of the propeller rotation. This important characteristic was found in a larger extent by Watanabe et al. (5) for a Propfan which interacts with the wake of a pylon.

At the moment we try to predict these characteristics of the directivity pattern using the FWH-equation (s. chapter 2.2.2). The important input for the dominant dipole terms are the distributions of the unsteady blade pressures. These are computed with the code described in chapter 2.1.

5. Noise of Propfans during take off and landing

The program system described in chapter 2 computes the noise field radiated by a single propeller. In order to extend the computation to a counter-rotating propeller system, two additional effects have to be included: the aerodynamic and the acoustic interferences between the two rotors. The former is caused by the fact that each of the rotors has to operate in a flow field which is influenced by the other rotor. This is especially of great importance for the aft rotor whose inflow contains the induced downwash and the viscous wakes of the forward rotor blades. The downwash can be predicted by a complex modeling of the vortex systems developed by Müller (14); the predicted downwash agrees very well with the measured values. The wakes of the forward rotor blades, originating from the boundary layers of the blades, are modeled using a theory of Silverstein et al. (15).

It is important to know how far an interfering wake is deformed by the forward rotor before the aft rotor interacts with the wake. To obtain first informations the following experiment was performed.

5.1 Preliminary investigations on wake deformation

Using the test set, descibed in chapter 3, the deformation of the wing wake passing through the rotor plane has been investigated for different parameters (rotor speed, flight speed, blade setting angle). Velocity measurements were carried out 0.165 m upstream and 0.123 m downstream of the rotor. Figure 5.1 shows the measured wakes at these two axial positions.

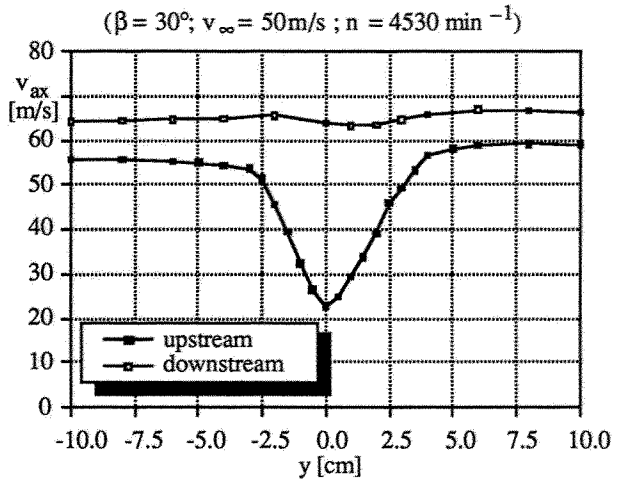

Fig. 5.1 Reduction of a wake by a rotor

The wake amplitude A is drastically reduced by the rotor. Since inside the wake the blade forces are increased, the flow experiences, by reaction, an additional acceleration which smoothes out the wake profile. As another effect, the rotor induces a swirl angle of 7° for the given configuration.

As described in chapter 4.1, a wake can be characterized, among others, by its loss of momentum I_0. Thus, I_0 is displayed in figure 5.2 for the upstream and downstream position as a function of rotor speed n and flight speed v_∞.

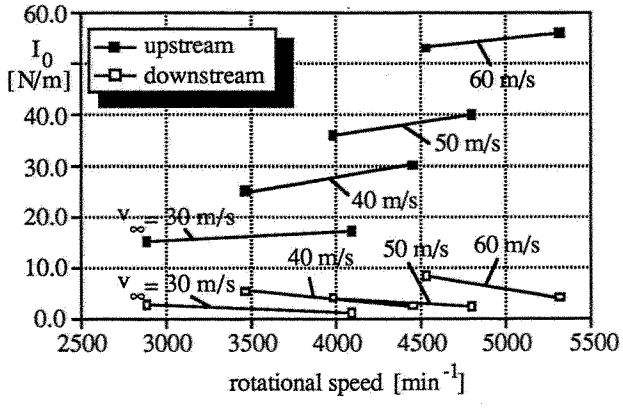

Fig 5.2 Reduction of I_0 by a rotor

Downstream of the rotor, I_0 is reduced almost to zero and the influence of v_∞ and n, which is considerable in the upstream region, is nearly negligible downstream of the rotor.

The results of these preliminary measurements lead to the conclusion that for a counter-rotating Propfan (CRP) the aft rotor is only slightly influenced by a wake in the inflow. However, the aft blades interact with the viscous wakes shed by the forward rotor blades.

5.2 Theoretical results

The calculation of the produced sound power of CRPs requires an integration of the sound pressures over a surrounding sphere. Since the aft rotor is located eccentric to this sphere, a modification of the noise calculation module LAERM was required. A further module has to be implemented to superimpose the noise fields of the two rotors.

Fig. 5.3 compares the emitted sound power levels for several Propfan configurations:

- a 10-bladed single rotating Propfan (SRP),
- a counter rotating Propfan (CRP) with 10 forward- and 10 aft blades (= CRP-1),
- a CRP with 9 forward- and 11 aft blades (= CRP-2) and
- a CRP with 10 forward- and 10 aft blades but with swept blades (= CRP-3).

All configurations have a diameter of 1.55 m, a tip Mach number $M_t = 0.8$ and the same values of total thrust and flight speed, v_∞=50 m/s (take off and landing). The distortion is generated by one wake over the rotor circumference with A = 20 m/s and I_0 = 115 N/m. The three bars for the CRP-configurations show the sound power levels of the forward fan (fw), the aft fan (aft) and the superposed noisefield respectively. The levels for homogeneous and distorted inflow are compared.

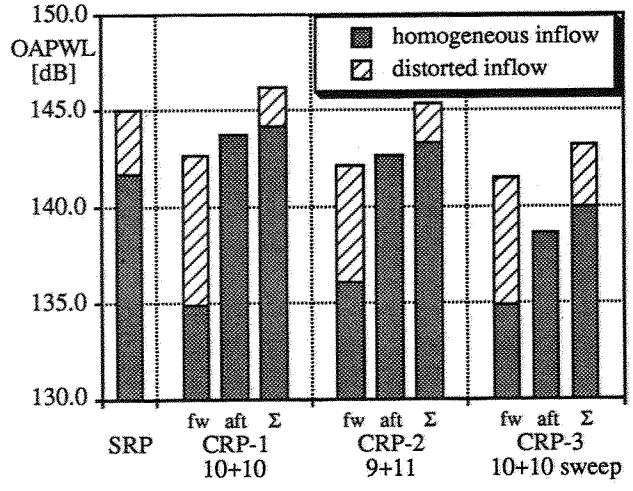

Fig. 5.3 Emitted sound power levels for different Propfan configurations

At first, the different levels for homogeneous inflow will be discussed. It can be stated that for every CRP-configuration the aft fan is the dominant noise source because of its distorted inflow due to the viscous wakes shed by the forward rotor blades. Its noise contribution exceeds that of the forward fan by values up to 9 dB. Comparing the different configurations mutually, the CRPs with unswept blades have remarkably higher levels than the configuration with swept blades. The CRP with swept blades has the lowest noise levels. For CRP1 all aft blades interact with all wakes of the front blades at the same time, while for CRP2 the interactions take place at different times. That leads to a noise reduction of CRP2 in the range of 1 dB compared to CRP1. The sweep back of the blades (CRP3) has a significant influence on the noise emission. The resultant power level is 4.2 dB lower than that of CRP1 (having the same blade numbers). This can be explained by the fact that the several radial parts of an aft blade interact at different times with the wake of a forward blade. In this way the impulsive character of the sound radiation of the aft fan is reduced and the higher harmonics in the sound spectrum have lower levels.
If the inflow is distorted, only the noise level of the forward fan of the CRPs is increased because of the assumption that the aft

rotor is not influenced by the wake (s. chapter 5.1). The total level is increased by up to 3 dB.

6. Conclusions

For take off and landing configurations, the noise radiation of propellers and Propfans, influenced by inflow distortions (wakes of e.g. pylons or wings), is investigated theoretically and in experiments. The Fourier-coefficients and the phase relations of the unsteady blade forces, generated at the rotor blade elements, are the important input to the noise computational program.

- For low rotational tip Mach numbers in the range of $M_t = 0.4$, the radiated noise is highly influenced by the inflow distortions. The maximum increase of the noise power level of a 5-bladed rotor whose blades cut one wake per revolution is in the range of more than 30 dB during take off! The lift coefficient of the blades is $c_L = 0.7$.
- With increasing M_t the steady blade forces get more influence on the noise radiation due to the higher values of their Bessel-functions. This means that the influence of inflow distortions is reduced. At $M_t = 0.95$, typical for Propfans, the noise power level is increased by not more than 3 dB, if one strong wake penetrates the rotor plane ($c_L = 0.7$).
- The maximum increase of the noise power levels occurs if the width of the wake is 1/3 of the propeller diameter (see figures 4.5 to 4.8).
- Loss of momentum I_0 and defect amplitude A of the wake are the most important factors influencing the additional noise emission. For small values of I_0 the influence of I_0 predominates while for higher values of I_0 the influence of the amplitude is prevailing.
- A propeller whose inflow is homogeneous has a noise spectrum with steeply decreasing higher harmonics of the blade passing frequency. But for a propeller with disturbed inflow, many of higher sound harmonics grow to considerable levels increasing the overall sound power level. For higher values of M_t, an increased number of blade force harmonics contribute strongly to the sound harmonics.
- The circumferential noise pattern of the propeller shows that the sound radiation is turned, relative to the position of the wakes, into the direction of the propeller rotation.
- To reduce the noise emission of a propeller for a given thrust with distorted inflow, it is favourable to choose high effective angles of attack and low tip Mach numbers. (The predicted noise levels are in good agreement with the measurements).
- Many methods for reducing the noise, caused by inflow distortions, have been tested. Promising is the use of propellers whose blades have swept planform. Because the radial parts of every blade interact at different times with the wake, the impulsive character of the radiated noise is reduced. For the tested configuration, the noise power level was decreased by about 3 dB. For Propfans the same mechanism is acting (s. below). As another successful way, special guide vanes, installed just before the trailing edge of the wake-generating body, provided good results.
- An experimental investigation for counter-rotating Propfans (CRP) for takeoff conditions showed that a wake in the inflow is reduced by the forward rotor in such an extent that the aft rotor is barely influenced by the wake.
- For CRPs with homogeneous inflow the aft rotor is always the dominant noise source because of the interaction with the viscous wakes shed by the forward blades. If the inflow is distorted by a wake, their amplitude is diminished by the forward rotor and has only a slight influence on the aft rotor. Thus, the forward rotor can be the stronger noise source. A swept blade planform decreases the additional noise emission caused by inflow distortions and by the interaction between forward and aft rotor.

7. References

1 Kellner, A., "Experimentelle und theoretische Untersuchungen über den Einfluß inhomogener Geschwindigkeitsverteilung in der Zuströmung auf die Lärmerzeugung von Mantelschrauben", Ph. D. Thesis, RWTH Aachen, 1980

2 Schreier, J., "Experimentelle und theoretische Untersuchungen der Schallabstrahlung von Rotoren und Propellern, die sich in Wirbelfeldern bewegen", Ph. D. Thesis, RWTH Aachen, 1983

3 Neuwerth, G., Staufenbiel, R., Kellner, A., Schreier, J., "Fluctuating Forces and Rotor Noise due to Distorted Inflow", ICAS-Proceedings, pp. 674-688, 13. ICAS Congress, Seattle, USA, 11.-27.8.82

4 Magliozzi, B., "Noise Characteristics of Model Counter-Rotating Prop-Fans", AIAA-87-2656

5 Watanabe, T., Kawachi, K., Nakamura, Y., "Noise Prediction of a Counter-Rotation Propfan", Journ. of Aircraft, Vol. 26, No. 12, Dec. 1989

6 Neuwerth, G., Müller, R., "Pressure Fluctuations on Rotor Blades Generated by Blade-Vortex Interaction", Vertica, Vol. 9, Nr. 3, pp. 227-239, 1985

7 Kemp, H.H., Sears, W.R., "The Unsteady Forces Due to Viscous Wakes in Turbomachines", Journ. Aeron. Sci., Vol. 22, pp. 478-483, 1955

8 Horlock, J.H., "Fluctuating Lift Forces on Airfoils Moving through Transverse Chordwise Gusts", Journ. Basic Engineering, Vol. 90, Ser. D Nr. 4, pp. 494-500, 1968

9 Naumann, H., Yeh, H., "Lift on Pressure Fluctuations of a Cambered Airfoil under Periodic Gusts and Applications in Turbomachinery", Paper 72-GT-30, ASME, 1972

10 Lighthill, M.J., "On Sound Generated Aerodynamically", Proc. Roy. Soc., A 211, pp 564-587, 1952

11 Lowson, M.V., "Theoretical Studies of Compressor Noise", NASA CR-1287, 1969

12 Ollerhead, J.B., Munch, C.L., "An Application of Theory to Axial Compressor Noise", NASA CR-1519, 1970

13 Wright, S.E., "Discrete Radiation from Totating Periodic Sources", Journ. Sound Vibr., Vol. 17, pp. 437-498, 1971

14 Müller, R.H.G., Staufenbiel, R., "The influence of winglets on rotor aerodynamics", Vertica, Vol. 11, No. 4, pp. 601-618, 1987

15 Silverstein, A., Katzoff, S., Bullivant, W.K., "Downwash and Wake Flow Behind Plain and Flapped Airfoils", NACA Tech. Rept. No. 651, 1939